2014

The 17 May 2012 M4.8 earthquake near Timpson, East Texas: An event possibly triggered by fluid injection

Cliff Frohlich
University of Texas at Austin

William Ellsworth
Earthquake Science Center, U.S. Geological Survey

Wesley A. Brown
Stephen F Austin State University, brownwa1@sfasu.edu

Michael Brunt
Eagle Pass High School

Jim Luetgert
Earthquake Science Center, U.S. Geological Survey

See next page for additional authors

AGU PUBLICATIONS

JGR

Journal of Geophysical Research: Solid Earth

RESEARCH ARTICLE
10.1002/2013JB010755

Key Points:
- The 17 May 2012 earthquake is the largest recorded historically in east Texas
- Its best-located aftershocks lay along a plane and had depths of 1.6-4.6 km
- Fluid injection at nearby disposal wells probably triggered these earthquakes

Supporting Information:
- Readme
- Figure S1
- Table S1
- Table S2
- Table S3

Correspondence to:
C. Frohlich,
cliff@ig.utexas.edu

Citation:
Frohlich, C., W. Ellsworth, W. A. Brown, M. Brunt, J. Luetgert, T. MacDonald, and S. Walter (2014), The 17 May 2012 *M*4.8 earthquake near Timpson, East Texas: An event possibly triggered by fluid injection, *J. Geophys. Res. Solid Earth*, *119*, 581–593, doi:10.1002/2013JB010755.

Received 4 OCT 2013
Accepted 2 JAN 2014
Accepted article online 6 JAN 2014
Published online 29 JAN 2014

The 17 May 2012 *M*4.8 earthquake near Timpson, East Texas: An event possibly triggered by fluid injection

Cliff Frohlich[1], William Ellsworth[2], Wesley A. Brown[3], Michael Brunt[4], Jim Luetgert[2], Tim MacDonald[2], and Steve Walter[2]

[1]Institute for Geophysics, University of Texas at Austin, Austin, Texas, USA, [2]Earthquake Science Center, U.S. Geological Survey, Menlo Park, California, USA, [3]Department of Geology, Stephen F. Austin State University, Nacogdoches, Texas, USA, [4]Eagle Pass High School, Eagle Pass, Texas, USA

Abstract This study summarizes our investigation of the 17 May 2012 $M_{W\text{-RMT}}$4.8 earthquake near Timpson, Texas, the largest earthquake recorded historically in eastern Texas. To identify preshocks and aftershocks of the 17 May event we examined the arrivals recorded at Nacogdoches (NATX) 30 km from the 17 May epicenter, at nearby USArray Transportable Array stations, and at eight temporary stations deployed between 26 May 2012 and mid-2013. At NATX we identified seven preshocks, the earliest occurring in April 2008. Reliably located aftershocks recorded by the temporary stations lie along a 6 km long NW-SE linear trend corresponding to a previously mapped basement fault that extends across the highest-intensity (MMI VII) region of the 17 May main shock. Earthquakes in this sequence are relatively shallow—with focal depths ranging from 1.6 to 4.6 km. Evidence supporting these depths include: hypocentral locations of exceptionally well-recorded aftershocks, *S-P* intervals at the nearest stations, and comparisons of synthetics and observed seismograms. Within 3 km of the linear trend of aftershock activity there are two Class II injection disposal wells injecting at 1.9 km depth beginning in August 2006 and February 2007, with injection rates averaging 42,750 m^3/mo and 15,600 m^3/mo, respectively. Several observations support the hypothesis that fluid injection triggered the Timpson sequence: well-located epicenters are situated near a mapped basement fault and near high-volume injection wells, focal depths are at or below the depths of injection, and the earliest preshock (April 2008) occurred after the onset of injection in 2006.

1. Introduction

On 17 May at 0812 UTC a $M_{W\text{-RMT}}$4.8 earthquake occurred near Timpson, Texas. The quake awoke numerous residents of Nacogdoches, Texas, 50 km to the southwest of Timpson and caused significant damage to chimneys, fireplaces, and brick veneer siding 5 km southwest of Timpson. The 17 May earthquake is the largest earthquake in the historical record in East Texas (Figure 1). This paper discusses this earthquake and the sequence of preshocks and aftershocks, including an $M_{W\text{-RMT}}$4.0 foreshock on 10 May 2012 at 1515 UTC and aftershocks occurring on 25 January 2013 at 701 UTC (m_{bLg}4.1) and 2 September 2013 at 1652 (m_{bLg}4.1) and 1851 ($M_{W\text{-RMT}}$4.3).

Regional tectonics in eastern Texas is dominated predominately by salt bodies; however, the Mt. Enterprise fault zone, a system of approximately east–west trending Cretaceous-Paleogene faults, is situated north and west of the epicentral area (Figure 1) [see *Ewing*, 1990]. In the epicentral area of the 2012 earthquake *Jackson* [1982] and *Geomap Company* [2012] also indicate a northwest-southeast trending fault that is roughly parallel to and slightly east of the Rusk-Shelby county line.

Seismicity was rare in this region prior to the events analyzed in this study. The nearest events discussed by *Frohlich and Davis* [2002] were a *M*4.0 8 January 1891 Rusk, Texas, event, 80 km to the west of the epicentral region and the *M*3.0 9 June 1981 Center, Texas, earthquake, 25 km to the southeast. However, some investigations have suggested the 1891 Rusk event might be spurious—a thunderstorm or a tornado—and the 1981 Center earthquake was only locatable because it was recorded by a temporary local network deployed between June 1981 and August 1982 [*Pennington and Carlson*, 1984]. This network also recorded a microearthquake occurring on 11 December 1981 and located 25 km west of the 2012 epicenter.

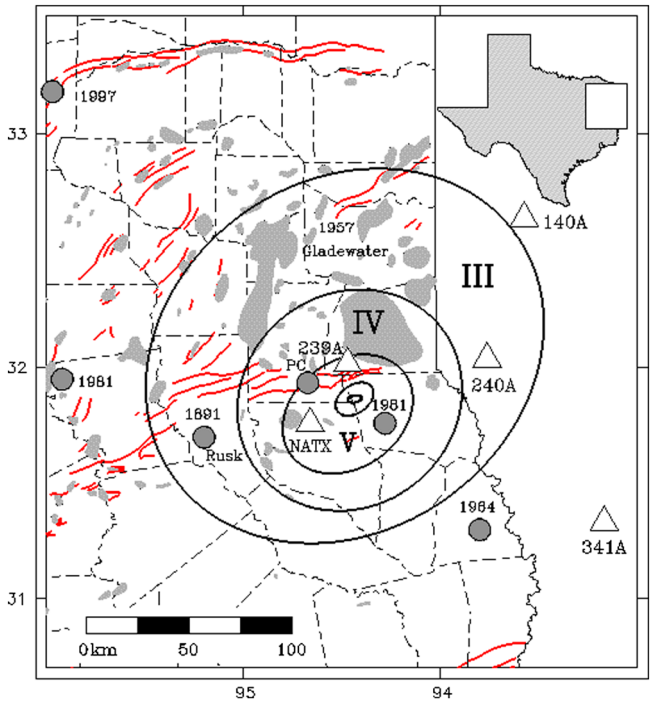

Figure 1. Felt area of 17 May 2012 $M_{W\text{-}RMT}$4.8 earthquake. Roman numerals indicate regions experiencing modified Mercalli intensities MMI III, MMI IV, and MMI V; unlabeled regions within MMI V ellipse experienced MMI VI and MMI VII. Grey circles are historically reported earthquakes from *Frohlich and Davis* [2002]; labels indicate year of occurrence. Also plotted and labeled "PC" is 11 December 1981 microearthquake located by *Pennington and Carlson* [1984]. Red lines are regional faults as mapped by *Ewing* [1990]; the fault system north and west of the highest-intensity region is the Mt. Enterprise fault zone. Triangles are regional seismic stations nearest the 17 May epicenter; all but 239A, which closed December 2011, were used to locate it. Gray shaded regions are oil and gas fields as described by *Galloway et al.* [1983] and *Kosters et al.* [1989]. Dashed lines are county boundaries. Rectangle within Texas icon at upper right indicates area mapped in this figure.

There are two high-volume injection disposal wells within 3 km of the highest-intensity region of the Timpson earthquakes, and it is possible that injection triggered them. Since 2008, fluid injection appears to have triggered several earthquake sequences in Texas and elsewhere in the Midwestern U.S. [*Frohlich et al.*, 2011; *Frohlich*, 2012; *Horton*, 2012; *Keranen et al.*, 2013; *Ellsworth*, 2013; *Justinic et al.*, 2013].

We first present results from a felt report survey for the 17 May 2012 earthquake. We then summarize our analysis of seismograms to identify and locate earthquakes in the sequence; nearby stations include U.S. National Network station NATX in Nacogdoches located 25 km from the epicenter, several nearby EarthScope Transportable Array stations, and eight temporary seismographs deployed following the 17 May earthquake. Finally, we describe the injection disposal wells situated near the epicentral area and discuss their possible relationship with seismicity.

2. Felt Reports From the May 2012 Earthquakes

The 10 May foreshock and 17 May main shock were strongly felt in the region around Timpson, TX, with the area of high intensities including the zip code for the town of Garrison to the southwest. Instrumental epicenters determined by the USGS, however, place the foreshock 10 km northwest of Timpson and the main shock 4 km to the northeast (Figure 2). The ~10 km difference in their epicenters is consistent with the formal uncertainty in their locations, suggesting that they might be nearly colocated (as we might expect). To better constrain the epicentral area of these events we gathered felt report information (Figures 2 and 3) from three different sources. Following the 17 May earthquake, we contacted the *Nacogdoches Daily Sentinel* and the *Timpson and Tenaha News*, who published felt report questionnaires that respondents mailed either to us or to newspaper offices. Two of the authors (M.B. and W.A.B.) spent 3 days in the epicentral region interviewing residents, concentrating their efforts in the higher-intensity areas.

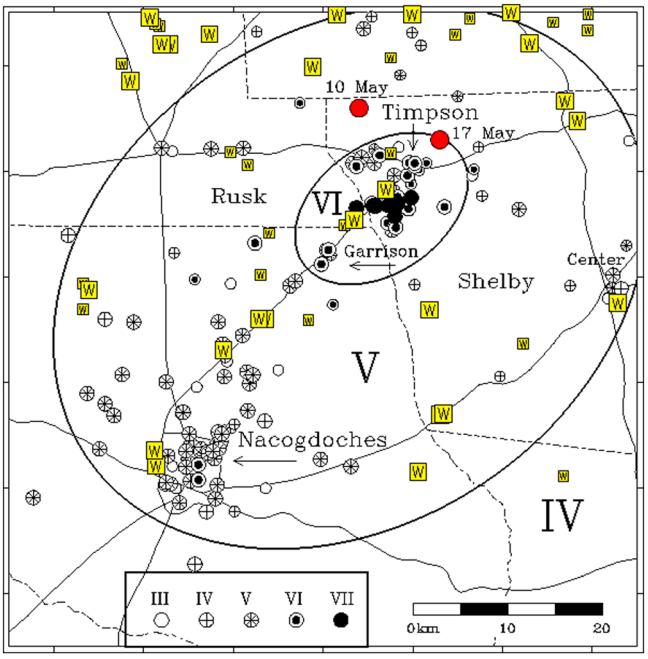

Figure 2. Locations of felt reports for the 17 May 2012 earthquake. Key at bottom of figure shows symbols for felt intensities MMI III to MMI VII; larger symbols are reports collected by the authors; smaller symbols are DYFI reports provided by the NEIC. Yellow squares labeled "W" indicate the location of Class II injection wells; larger (smaller) symbols are wells with maximum monthly injection volumes exceeding (less than) 100,000 BWPM (16,000 m^3/mo). Red circles are NEIC epicenters determined for the 10 May and 17 May 2013 earthquakes. Solid lines are regional roads; broken lines are county boundaries.

We augmented these data with "Did you feel it?" (DYFI) information provided by the National Earthquake Information Center (NEIC). The DYFI program [*Atkinson and Wald*, 2007; *Wald et al*., 2011] is an internet-based program where individuals can provide unsolicited responses to questions about their experiences and location during an earthquake. The responses are analyzed to assign a modified Mercalli intensity (MMI) value; the NEIC routinely presents summary online maps of the MMI distributions. For this study the DYFI data were especially useful for constraining boundaries for the MMI III and MMI IV regions (Figure 1).

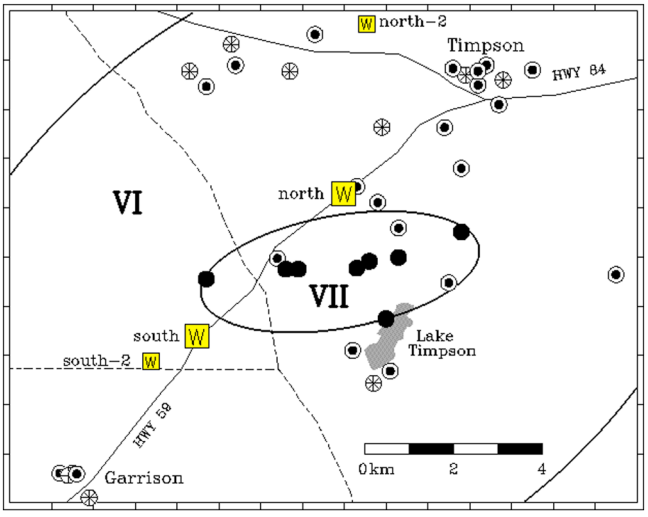

Figure 3. Locations (circles) of felt reports and injection wells (squares) near the 17 May 2012 epicenter. County lines, highways, and key for MMI level are as in Figure 2. Ellipse labeled "VII" shows approximate extent of MMI VII area. Squares labeled W are locations of Class II injection disposal wells. The town of Timpson is at the junction of state highways 59 and 84.

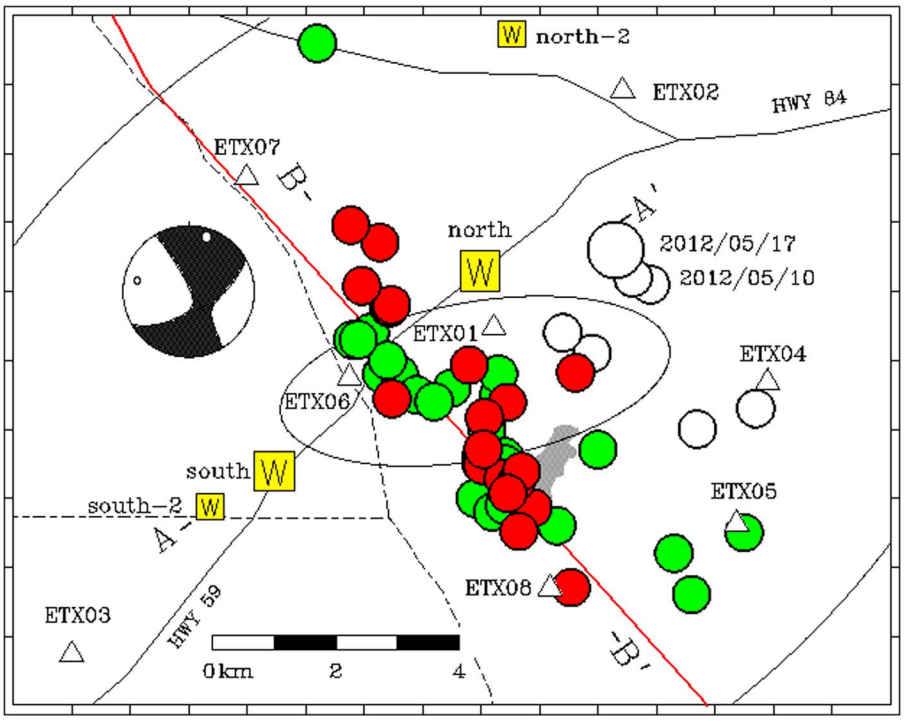

Figure 4. Epicenters (circles) determined in this study (see Table S2). White circles are epicenters occurring before 26 May 2012 when the first temporary stations (triangles) were deployed. Green circles are epicenters occurring between 26 May 2012 and 5 February 2013; red circles are best-recorded hypocenters occurring after 22 February 2013. Red line indicates basement fault from *Jackson* [1982]. Yellow squares labeled W are locations of injection disposal wells as in Figures 2 and 3. Ellipses indicate MMI VI and MMI VII areas as in Figure 3. Beach ball is global centroid moment tensor reported by Columbia group (see www.globalcmt.org); note that the best recorded hypocenters (red circles) lie along a NW-SE trend approximately parallel to one nodal plane. Labels A, A', B, and B' indicate locations of cross sections (Figure 6).

We interviewed residents at eight locations who experienced the most severe intensities (MMI VII); these occurred within a 5.7 km × 2.3 km area (~10 km^2) about 6 km southwest of Timpson, TX, in the direction of Garrison (Figure 3). These individuals reported significant damage to chimneys, fireplaces, or masonry; objects such as pictures, mirrors, or deer heads fell off walls; objects fell off shelves or out of cabinets and often broke. One respondent reported his fireplace came down inside his residence, and his south exterior brick wall "blew off" the house.

People experienced intensities of MMI VI and MMI V over areas of approximately 170 km^2 and 2200 km^2, respectively. Since the earthquake occurred at 3:12 A.M. local time, in the MMI V region typical respondents noted that they were awakened by the earthquake and realized that furniture was moving or objects were rattling. The MMI IV and MMI III felt areas covered approximately 7000 km^2 and 20,000 km^2, respectively.

We also collected felt report information for the 10 May M_W3.9 earthquake. This was much less severe than the 17 May earthquake and took place in the morning, 10:15 local time. Several residents of Timpson and the region approximately 5–10 km to the southwest experienced intensities of MMI V; the region of highest intensity for the 10 May event coincided roughly with the highest-intensity region for the 17 May main shock.

3. Analysis of Seismograms: Origin Times and Epicenters

3.1. Seismic Station Coverage

Seismic station coverage in this part of East Texas has varied considerably over the past few years (Table S1 in the supporting information). The nearest permanent seismic station is the U.S. National Network station NATX in Nacogdoches, operational since 2004 and situated approximately 25 km southwest of the highest-intensity region (Figure 1). Between 2009 and 2011 EarthScope USArray Transportable Array (TA), stations were deployed in eastern Texas; until December 2011 TA station 239A operated 15 km north of the epicentral region. TA stations 140A, 240A, and 341A were installed some 65–140 km to the east between February 2011

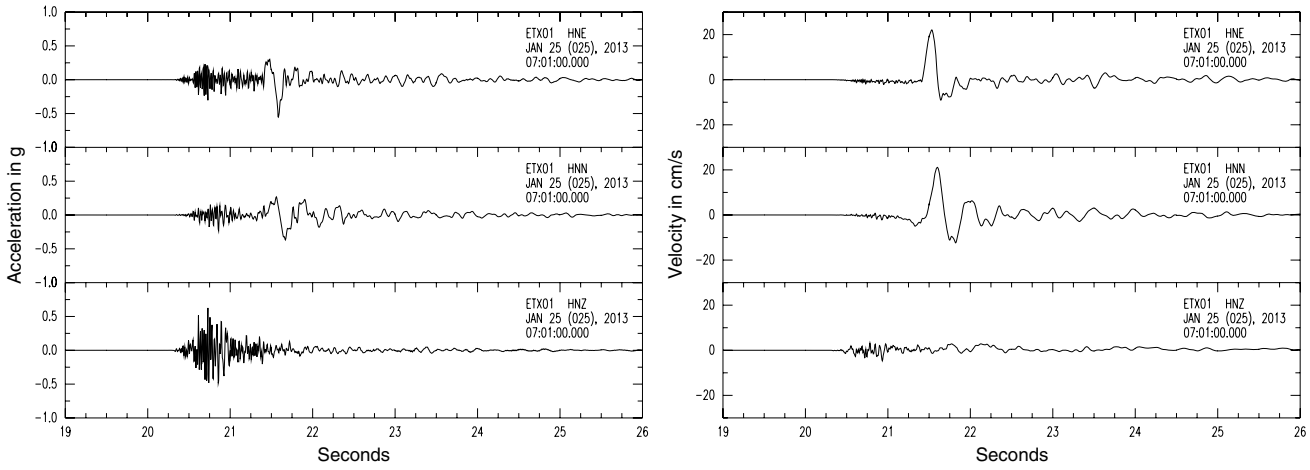

Figure 5. Accelerations (left) and velocities recorded at ETX01 for the 25 January 2013 0701 UTC m_{bLg}4.1 aftershock. The 1.08 s *S-P* time at this closest station to the event requires a shallow focal depth for the earthquake.

and February 2012. Because of the absence of stations in the epicentral area, we fixed focal depths at 2.5 km to locate earthquakes occurring prior to 26 May 2012 (white circles in Figure 4) and their epicentral uncertainties are several km. In particular, for the 2011 to May 2012 earthquakes in Table S2, our relocations found a median value for the largest axis of the uncertainty ellipse to be ±2.9 km.

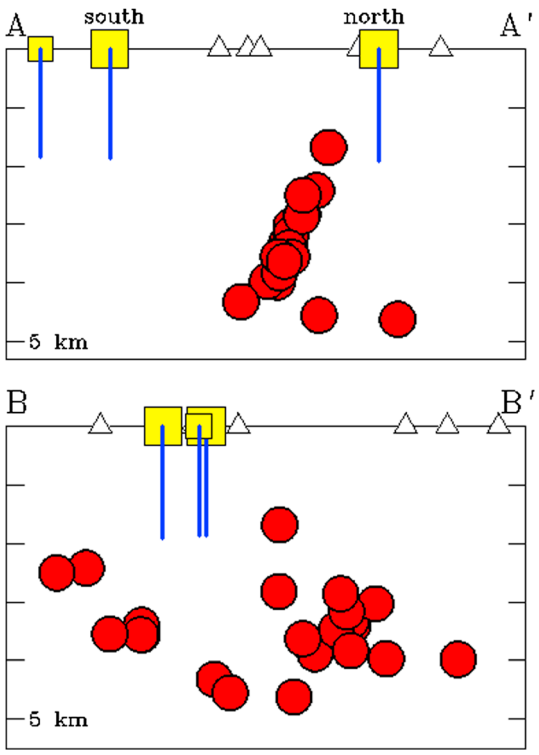

Figure 6. Cross sections A-A′ and B-B′ (see Figure 4) of best recorded hypocenters (red circles) determined in this study. Symbols are as in Figure 4; blue lines extending beneath injection wells (yellow squares) indicate depth extent of injection wells. Note that hypocenters in section A-A′ form a linear group extending from ~1.5 to 4.5 km depth, suggesting they may occur along a southwest dipping planar surface trending ~35° west of north.

Following the 17 May 2012 earthquake we installed three temporary NetQuakes accelerometers (ETX01, ETX02, and ETX03; see Figure 4 and Table S1) between 26 May and 15 June. Because these instruments required access to power and an internet connection, we only were able to find sites for them along HWY 59 between Nacogdoches and Timpson. Thus, for aftershocks occurring between 26 May 2012 and February 2013, the stations closest to the highest-intensity region (NATX, ETX01, ETX02, and ETX03) were situated approximately along a northeast trending straight line. Two stations somewhat to the east (140A and 240A) lay approximately along an extension of this line. Thus, arrivals at the remaining, relatively distant station 341A (distance ~ 1.2°) were critical for constraining aftershock locations along the northwest-southeast direction. There were readable *P* and *S* phases at 341A for only three earthquakes detected during the 26 May 2012 to February 2013 period. For earthquakes during this period we determined locations (green circles in Figure 4) with focal depths fixed at 2.5 km, and their epicentral positions along the NW-SE direction are poorly determined.

The region was shaken strongly a third time on 25 January 2013 at 0701 UTC by a m_{bLg}4.1 aftershock. This event was well recorded by the three NetQuakes accelerometers. Peak acceleration and peak velocity at the closest instrument ETX01 were 62% of gravity and 22 cm/s, respectively (Figure 5).

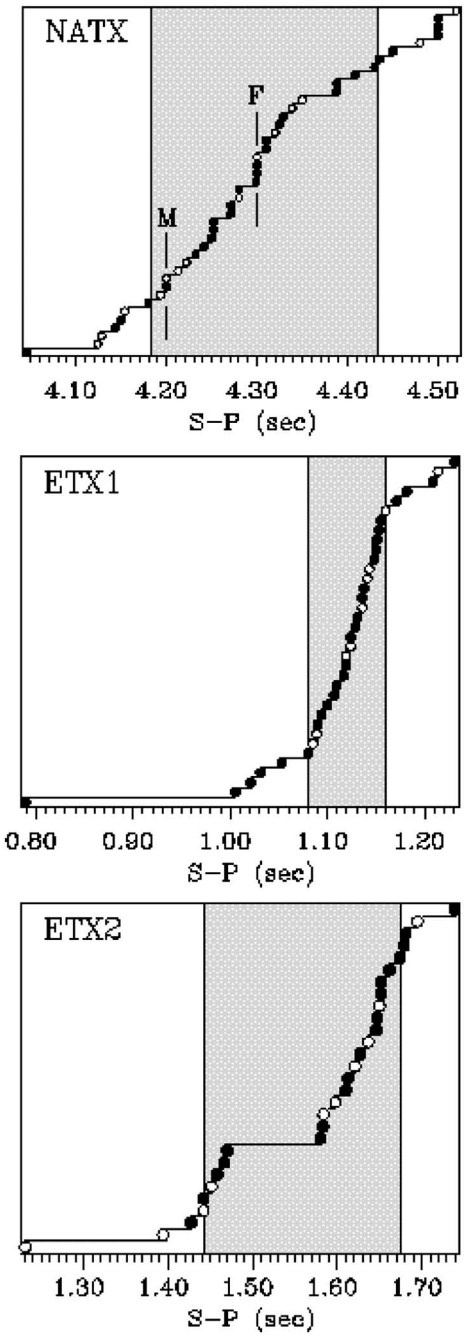

Figure 7. Cumulative distribution of *S-P* intervals observed at three stations recording the Timpson sequence. Open circles indicate less-reliable data where either the *S* or *P* reading was of lower quality. Grey area between vertical lines indicates the middle two thirds of the distribution. (top) *S-P* intervals at station NATX; times labeled M and F are *S-P* intervals for 17 May 2012 main shock and 10 May 2012 foreshock. (middle) *S-P* intervals at ETX01. The observation that *S-P* intervals are ~1.1 s indicates focal depths must be ~4 km or shallower (see text). (bottom) *S-P* intervals at ETX02. The observation that *S-P* intervals form two groups suggests that the earthquakes originate from at least two distinct clusters.

In response to this earthquake we installed five additional stations (ETX04–ETX08, see Figure 4) equipped with both broadband seismometers and accelerometers to surround the epicentral area. These stations were operational starting on 22 February 2013 and remained in the field until early August 2013. For this paper, we have analyzed a subset of the earthquakes recorded by the combined network of temporary stations and NATX to determine hypocenters with free depths (red circles in Figures 4 and 6). We consider the epicentral locations and focal depths to be reliable for these events because they are located within the network—median values are ±0.3 km for the largest axis of the epicentral uncertainty ellipsoid and ±0.6 km for focal depth. These error estimates refer to the precision of the relative location only, as we lack a calibration shot to constrain the absolute location uncertainty. Absolute errors are likely less than 1 km, considering the network geometry, timing precision, and uncertainty in crustal velocity model.

On 2 September 2013 two more earthquakes occurred, at 1652 UTC with m_{bLG}4.1 and at 1851 UTC with $M_{W\text{-}RMT}$4.3. Because ETX04–ETX08 had been removed, we do not have accurate locations for these events. However, they are clearly in the same epicentral zone as the earlier events, with *S-P* times of ~1.0 s at ETX01. These earthquakes also produced excellent records at NATX that we have modeled to evaluate focal depth (see section 3.4).

3.2. Foreshocks and Aftershocks; (*S-P*) Times

NATX is the only regional station that has been continuously operational for more than 2 years. Using a seismogram from the 10 May 2012 event as a cross-correlation template, we searched NATX records from January 2005 to May 2012 and identified seven preshock events with magnitudes 0.5–2.2 (Table S2). All the events found had (*S-P*) times of 4.0–4.5 s at NATX (Figure 7, top), similar to that of the 10 May 2012 foreshock and the 17 May 2012 main shock, which had (*S-P*) times of 4.30 and 4.20 s, respectively. The earliest event (with *S-P* of 4.35 s) occurred in April 2008 and apparently went unnoticed by local residents.

For all Timpson earthquakes recorded by NATX we determined magnitudes (see Table S2). We performed a linear least squares fit between the logarithm of the peak-to-peak amplitudes and NEIC-reported magnitudes for 10 of the Timpson earthquakes reported by the NEIC. A frequency-

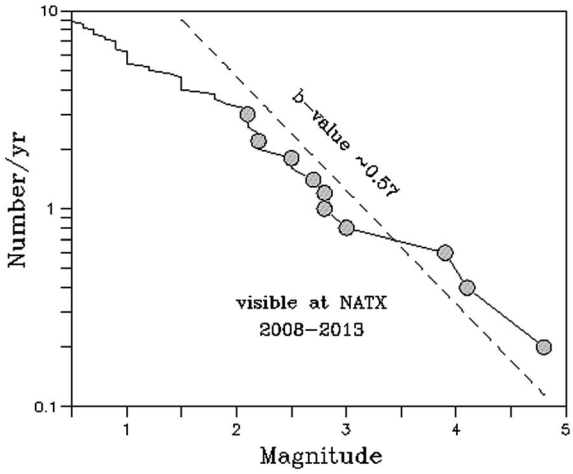

Figure 8. Magnitude distribution of Timpson earthquakes recorded at station NATX. Circles indicate events assigned magnitudes by NEIC; other magnitudes are as determined in this study.

magnitude plot of these data (Figure 8) indicates that NATX detects all Timpson earthquakes with magnitudes of ~2.0 and greater. The *b* value for the sequence is 0.570 ± 0.17 (95% confidence interval) as determined using *Aki*'s [1965] method for events having magnitude of 2.0 and larger.

In the year following the 17 May 2012 main shock we recorded 55 aftershocks; many were well recorded on the temporary stations ETX01 and ETX02. At ETX01, the station recording the smallest *S-P* intervals, all but one interval fell between 1.00 and 1.23 s (Figure 7, middle). At ETX02 the intervals formed two distinct groups (Figure 7, bottom), one clustered at 1.45 s and the other at 1.65 s.

3.3. Velocity Model and Locations

Historically, earthquakes have been rare in East Texas, and regional station coverage has been poor; thus, there is no well-established velocity model for location. For the 17 May 2012 earthquake the St. Louis group [see *Herrmann et al*., 2011] obtained a better fit to regional seismograms using their model WUS (western U.S.) than with model CUS (central U.S). In comparison with the CUS model, the WUS model has significantly lower velocities in the uppermost 8 km. Velocity logs for the depth interval ~1.0–3.5 km, including one well situated about 3 km north of the town of Timpson (API: 42–41931360), indicated that *P* velocity increased approximately linearly from about 3 km/s to 5 km/s in this depth range.

We developed a starting location model based on this information and then modified it to obtain a final model by applying the VELEST computer program to the best-recorded Timpson earthquakes (Group 3 in Table S2). VELEST solves the simultaneous hypocenter and 1-D velocity model tomography problem for local earthquakes as initial reference models for 3-D seismic tomography [*Kissling et al*., 1994]. Our final model (Table S3) has relatively low velocities with $V_P/V_S \sim 2$ to depths of 2.5 km and then $V_P/V_S \sim 1.72$ at greater depths. Because of the limited station coverage and relatively restricted range of focal depths, the model is determined only to about 4 km depth.

The deepest horizon plotted on *Jackson* [1982] summary cross sections of East Texas regional geology is the top of the Louann Salt at 4.5 km; the Louann is only a short distance above Paleozoic Ouachita basement. This is in general agreement with *Lutter and Novack*'s [1990] analysis of the Program for Array Seismic Studies of the Continental Lithosphere (PASSCAL) Ouchita experiment that found Mezozoic sediments extending to a depth of 5 km and also well logs shown by *Hammes et al*. [2011] from two wells about 20–30 km south of the 2012 epicenter.

For the 22 best-recorded earthquakes in Group 3, locations determined with this model had small residuals (average RMS error 0.02 s), with epicenters extending along a NW-SE line approximately 6 km long through the center of highest-intensity region (Figures 4 and 6, red circles). Focal depths are well constrained and ranged between 1.6 and 4.6 km. For our preferred velocity model (Table S3) the observed *S-P* intervals ranging from 1.0 to 1.2 s at ETX01 (Figures 5 and 7) are inconsistent with any focal depths exceeding 3.3–4.6 km.

We fixed focal depths at 2.5 km for the 30 epicenters in Group 2 (green circles in Figure 4). These were events with fewer observations at temporary local stations than the Group 3 earthquakes. Although the station distribution for Group 2 earthquakes provided relatively poor constraint along the NW-SE direction, our preferred locations were generally situated along the same NW-SE linear trend as the well-constrained Group 3 earthquakes.

Epicenters determined for earthquakes occurring before the installation of local stations (Group 1 in Table S2; white circles in Figure 4) were about 3 km east of the better-recorded events. These locations are not considered reliable; they are controlled by stations 140A and 341A situated 110–130 km east of the highest-intensity area; it is thus plausible that Group 1 locations are systematically mislocated by ~3 km as the velocity model is uncalibrated along their raypaths. The (*S-P*) intervals observed at station NATX for

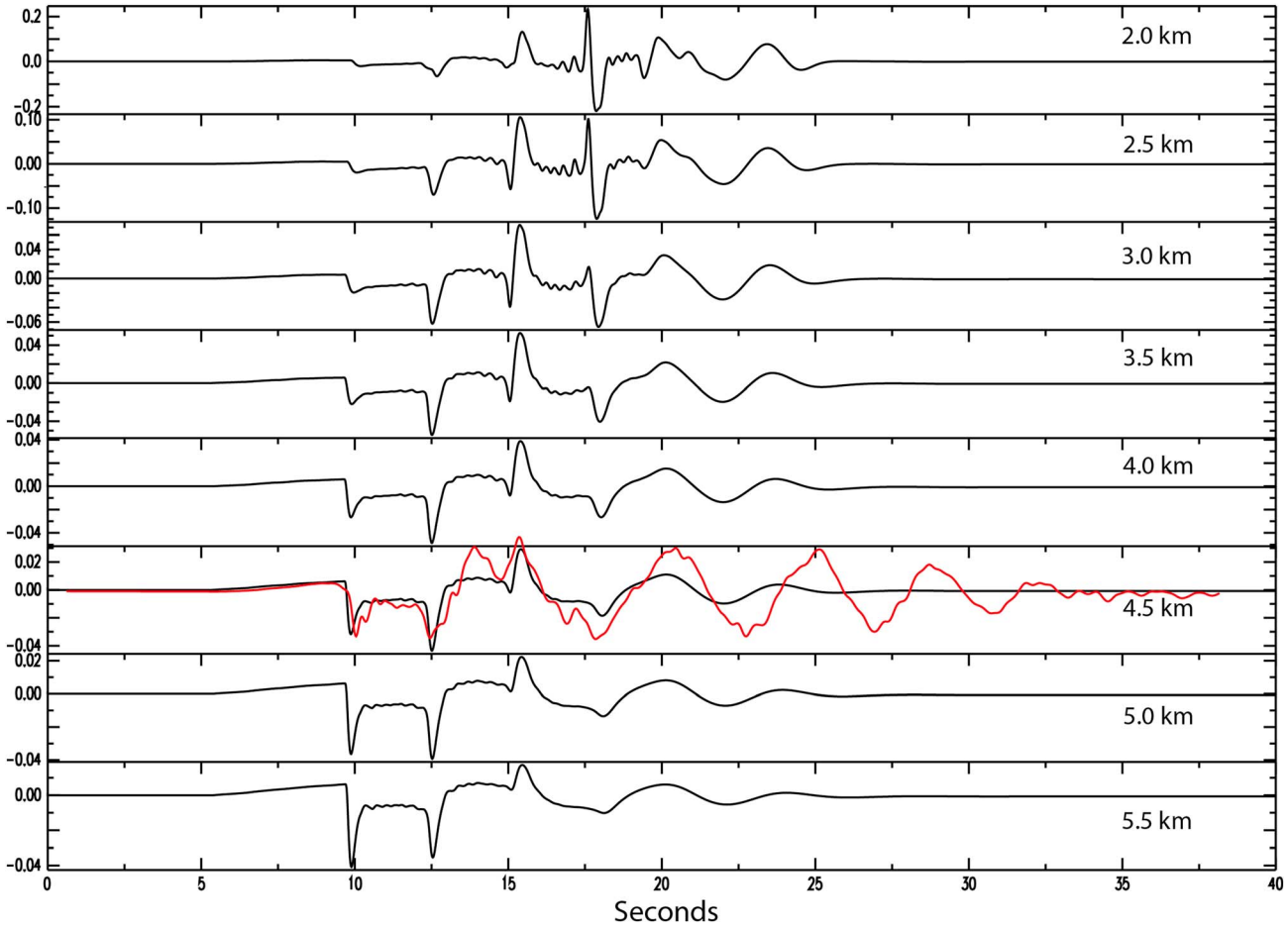

Figure 9. Transverse component displacement seismograms (black) for a double couple point source (strike = 330, dip = 85, rake = −15) at a range of 24.5 km and azimuth of 240° in the structure in Table S3 for depths between 2 and 5.5 km. The near-field ramp begins at the *P* wave arrival at approximately 5 s and is interrupted by the *S* wave arrival at approximately 10 s travel time. It is followed by multiple, impulsive arrivals, corresponding to whispering gallery arrivals from waves trapped in the sediments above basement. Note the sensitivity of the relative amplitudes of the whispering gallery phases to focal depth. Later arrivals have the largest amplitude at shallow depth, while the first arrival has the largest amplitude for deeper focal depths. Observed transverse displacement at NATX (red) for the 17 May 2012 main shock best matches a focal depth of 4.5 km. Both observed and synthetic displacements were low-pass filtered at 2 Hz.

Group 1 earthquakes, including the 10 May foreshock and 17 May aftershock, were similar to (*S-P*) intervals observed after installation of the local network (see Figure 7, top). This observation suggests that the Group 1 earthquakes occurred in nearly the same location as the later Group 2 and Group 3 events with better-constrained locations.

3.4. Modeling Seismograms Recorded at NATX

A notable feature of the transverse horizontal broadband seismograms recorded at NATX for the 17 May 2012 main shock are several high-amplitude phases arriving in the 20 s interval following the *S* arrival (Figures 9 and 10) on the transverse component of motion. Similar phases are visible on seismograms of the 10 May 2012 $M_{W\text{-RMT}}$3.9 and 25 January 2013 m_{bLg}4.1 earthquakes.

We interpret these arrivals as crustal reverberations—sometimes called "whispering gallery phases" [*Aki and Richards*, 1980] —generated when a shallow source lies near the boundary between a low-velocity gradient overlying a higher-velocity layer, and significant amounts of energy become trapped in the upper layer. We modeled the seismograms recorded at NATX for the 10 May 2012 foreshock, the 17 May main shock, the 25 January 2013 aftershock, and both 2 September 2013 aftershocks using the velocity model obtained with VELEST (Table S3) and the Global centroid moment tensor focal mechanism (Figure 4). Synthetic seismograms were computed using program FK [*Zhu and Rivera*, 2002] at the appropriate epicentral distance

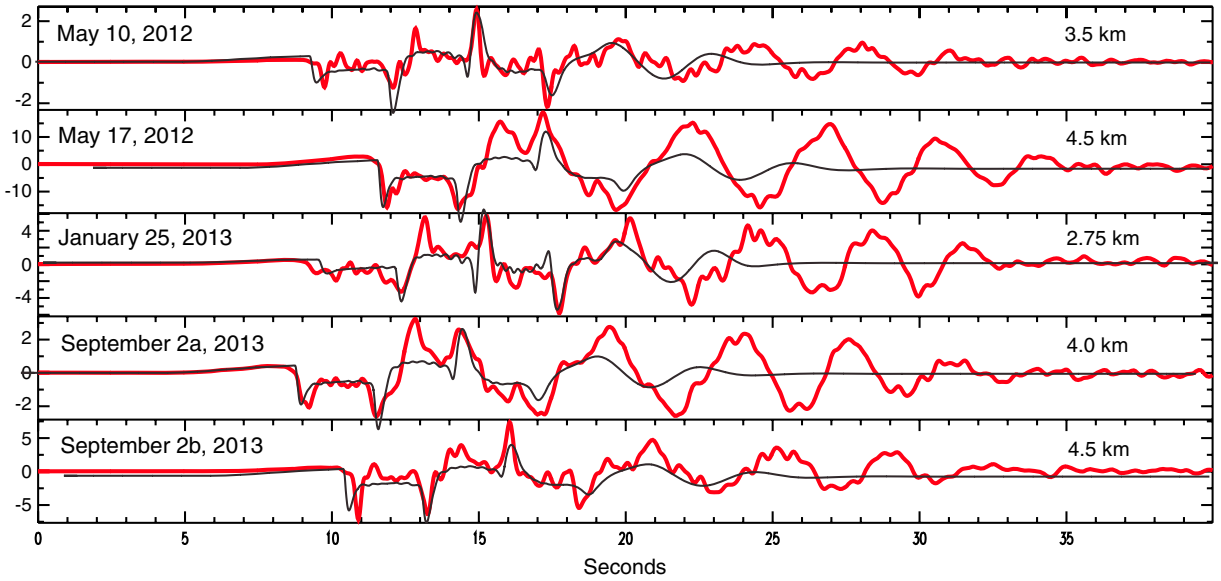

Figure 10. Transverse component displacement seismograms recorded at NATX (red) for the five principal earthquakes. Synthetic seismograms (black) are shown for the best fitting point source focal depth for the double-couple orientation used in Figure 9. Both observed and synthetic displacements were low-pass filtered at 2 Hz.

for a range of focal depths. Both the synthetic and observed seismograms were low-pass filtered at 2 Hz and integrated to displacement for comparison. We obtained the best match between the NATX displacement seismograms and the relative amplitudes of the whispering gallery phases for synthetic sources (Figure 9) at depths of 3.5, 4.5, 2.75, 4.0, and 4.5 km for these five events, respectively (Figure 10).

4. Injection Wells

In Texas, the Texas Railroad Commission (RRC), which no longer regulates railroads, is responsible for regulating activity related to petroleum operations in the state. The RRC issues permits for drilling wells and monitors production and underground disposal activities. By law operators annually provide the RRC with certain information concerning fluid injection, both when it is used to stimulate production and also when it is used to dispose of fluid wastes. The RRC's database is publically available online and includes information for individual wells and leases which is mostly complete for the past two decades; for each well the data include monthly volumes of water and gas injected and volumes of oil, water, and gas extracted.

Although East Texas has been the focus of recent unconventional gas development, in the immediate vicinity of the epicenters located in this study, there were no wells actively producing petroleum between 2000 and 2011 (see Figure S1). However, there were several such wells situated several kilometers to the southeast in Rusk and Nacogdoches Counties. Many of the gas wells began operation in 2005 or later and produced from formations within the Trinity at depths of 2.2–2.9 km.

There are, however, two relatively high-volume and two lower-volume injection disposal wells situated within several kilometers of the highest-intensity region of the 17 May 2012 earthquake (Figures 4 and 11). All four wells injected at depths of about 1.8–1.9 km; here Paleozoic basement is at ~5 km depth [*Jackson*, 1982; *Lutter and Novack*, 1990; *Hammes et al.*, 2011]. The highest injected volumes, averaging 269,000 barrels of water per month (BWPM) (42,750 m^3/mo) since September 2006, were at a well at 4 km southwest of the center of the MMI VII region (API 42–40133833; labeled "south" in Figure 4); RRC data indicates that injection was into the Rodessa of the Trinity formation. At a well about 2 km north of the MMI VII centroid (API 42–41931083; labeled "north" in Figure 4) monthly volumes averaged 98,000 BWPM (15,600 m^3/mo); injection here was also into the Rodessa. The total injected volumes for the north and south wells were 1.05 million m^3 and 2.90 million m^3, respectively.

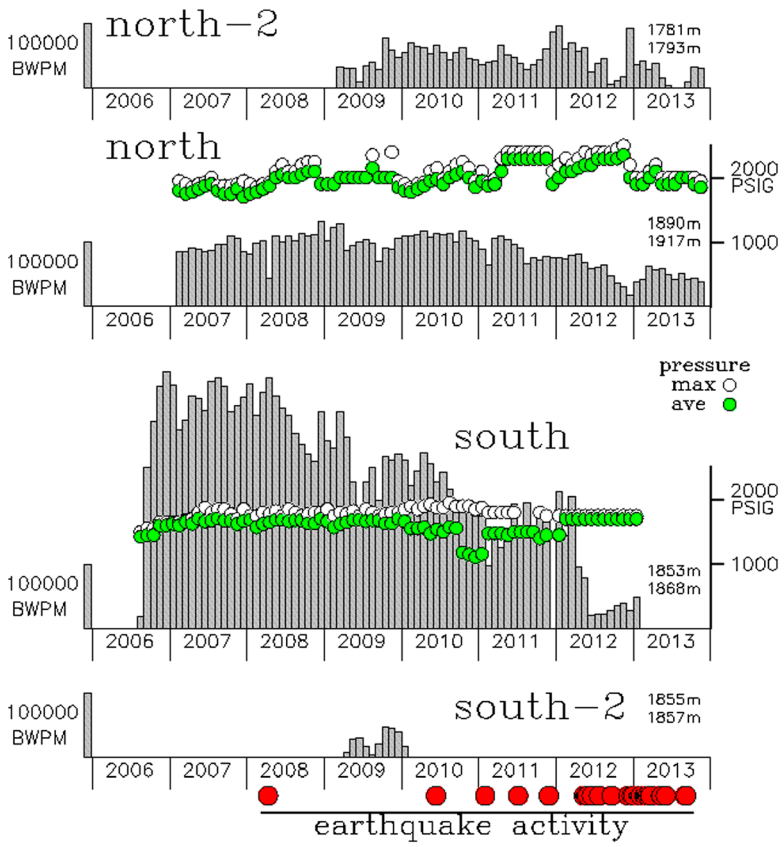

Figure 11. Monthly injection volumes for the wells indicated labeled north-2, north, south, and south-2 in Figure 4. Scale bar at left of histograms is 100,000 BWPM (16,000 m^3/mo). Green and white circles and right scale are average and maximum monthly injection pressures (1000 PSIG is 6895 kPa). Red circles indicate times of earthquakes identified in this study (see Table S2). Labels at right indicate depth interval of injection. At time of publication, information for February 2013 and later was not yet available concerning monthly injection volume and pressures for the south well.

While these are relatively high-volume wells, they are not unusual for Texas injection wells. There are more than 10,000 injection wells in Texas that have been active since 2000; of these more than 1300 have reported injection volumes exceeding 100,000 BWPM (16,000 m^3/mo) for 12 or more months since 2000.

Injection volumes were considerably less at two other regional wells. At well API 42–40131974 (labeled "south-2" in Figure 4) injection took place only from April 2009 to January 2010, and injection volumes never exceeded 50,000 BWPM (8000 m^3/mo). At a fourth well (API 42–41931287; labeled "north-2" in Figure 4) injection began in March 2009 and volumes averaged about 50,000 BWPM.

The RRC also reports monthly values for maximum and average injection pressures at disposal wells (Figure 11). At both the higher-volume wells, in 2010 and afterward, injection volumes decrease even as injection pressures hold steady, as at the south well, or increase, as at the north well. Variations in the injected volume presumably reflect demand and nothing more. Increasing injection pressure with decreasing volume injected could mean that the well bore has become constricted from a buildup of scale or plugging of a screen, or it could reflect increased resistance from the formation to accept additional fluid.

Modeling of subsurface hydrology and stress conditions in response to the pressure/volume histories at individual wells would help achieve a more complete understanding of the relationship between fluid injection and seismicity. However, this will require more information about injection pressures and well properties than is available from RRC data. The RRC-reported pressures are average and maximum surface pressures; these data do not reflect whether injection was episodic or continuous throughout the month. Moreover, the surface pressures for a pumping system do not account for frictional losses depending on casing diameters, etc., and thus are not related simply to the pressures at depth where well perforations permit fluid to disperse into subsurface strata.

5. Discussion

The most significant conclusions of the present study are that:

1. Epicenters of aftershocks of the 17 May 2012 earthquake occurred along a ~6 km long N35°W striking linear zone that coincides with a mapped basement fault [see *Jackson*, 1982; *Geomap Company*, 2012].
2. The epicentral area of aftershocks extends across the highest-intensity region of the 17 May 2012 $M_{W\text{-}RMT}$4.8 main shock, where local residents experienced intensities of MMI VII. Moreover, the aftershocks trend parallel to one nodal plane of the predominantly strike-slip focal mechanisms reported for this event by both the Columbia (Figure 4) and the St. Louis groups [*Ekström et al*., 2012; *Herrmann et al*., 2011].
3. The better-determined focal depths of sequence events are relatively shallow, with depths ranging from 1.6 to 4.6 km as determined by a network of temporarily deployed stations. For the five largest earthquakes in the sequence, modeling of the seismograms recorded at station NATX at a distance of 24.5 km indicates focal depths between 2.75 and 4.5 km.
4. Two relatively high-volume injection disposal wells are situated within ~3 km of the linear trend of epicenters and near the highest-intensity region of the 17 May main shock. Injection at these wells began in 2006–2007 prior to the first recorded sequence earthquake in April 2008.

5.1. Origin: Human-Triggered or Natural?

The above observations demonstrate that the Timpson earthquakes share many features in common with recent earthquakes elsewhere in the Midwestern U.S. that have been inferred to be triggered or induced. Like the 1962–1968 earthquakes in Denver [*Healy*, *et al*., 1968; *Herrmann and Park*, 1981], the 2008–2009 earthquakes in Dallas-Fort Worth [*Frohlich et al*., 2011], the 2009 earthquakes near Cleburne, TX, [*Justinic et al*., 2013] and the 2011 earthquake in Youngstown, OH [*Kim*, 2013], the Timpson earthquakes are the first known earthquakes in this location and began only after injection began. As in Denver, Dallas-Fort Worth, Cleburne, 2011 in Arkansas [*Horton*, 2012], and 2011 in Youngstown OH [*Kim*, 2013], the Timpson earthquakes had focal depths at or exceeding the depths of injection and occurred along a linear trend situated within only a few kilometers of the site of injection. Elsewhere in Texas, *Frohlich* [2012] found that seismic activity at distances of ~3 km is sometimes associated with wells having maximum monthly rates exceeding 150,000 BWPM (24,000 m^3/mo); in Timpson, injection rates averaged 269,000 BWPM (43,000 m^3/mo) since 2007 at the south well (Figures 4 and 11). All the above observations are consistent with the hypothesis that the Timpson earthquakes were triggered by nearby injection disposal wells; the likelihood that Timpson earthquakes are induced is comparable to that for the Denver, Dallas-Fort Worth, Cleburne, and Arkansas sequences.

Like the Dallas-Fort Worth earthquake sequence, the linear trend of aftershocks in Timpson approximately coincides with a mapped fault. In both cases we have been unable to locate the primary evidence confirming the faults' existence and location. The fault location indicated in Figure 4 is from *Jackson* [1982], as plotted on his map of faults at the top of Paleozoic basement; he does not place the fault on maps of faulting at shallower depths. *Geomap Company* [2012] shows the fault 2–3 km east of Jackson's location. The Timpson region has been the focus of recent exploration efforts, and we are seeking more recent data that might fix the location and dip of this fault, and thus resolve the possible discrepancy.

Although the preponderance of evidence favors the conclusion that the Timpson earthquakes were induced or triggered by fluid injection, our investigation cannot rule out the possibility that they are of natural origin. The historical record [*Pennington and Carlson*, 1984; *Frohlich and Davis*, 2002] indicates that in 1891 and 1981, well before injection began, *M*4.0 and *M*3.2 earthquakes occurred at Rusk, Texas, 80 km west of Timpson, and at Center, Texas, 25 km to the southeast (Figure 1). These could not have been triggered by human activity; rather, they have been attributed to the Mt. Enterprise fault zone (Figure 1). One of the focal planes for a focal mechanism reported for the 17 May 2012 earthquake (see Figure 4) is parallel to faults in the Mt. Enterprise fault zone as mapped by *Ewing* [1990]; the other focal plane is parallel to the mapped fault reported by *Jackson* [1982] and *Geomap Company* [2012].

5.2. Magnitude and Scalar Moment

The 17 May 2012 Timpson earthquake, with magnitude $M_{W\text{-}RMT}$4.8 and scalar moment M_o of 2.21×10^{23} dyn-cm, is the largest earthquake to have occurred in eastern Texas. The largest previous earthquakes in eastern and Central Texas are the 19 March 1957 *M*4.7 Gladewater earthquake, attributed to extraction in the East Texas oil field by several investigators, including *Frohlich and Davis* [2002] and the 20 October 2011 $M_{W\text{-}RMT}$4.8

Fashing earthquake (M_o 1.8×10^{23} dyn-cm), with an epicenter that coincides with several previous earthquakes that *Pennington et al.* [1986], *Davis et al.* [1995], and *Frohlich and Brunt* [2013] attributed to extraction in the Fashing gas field. The nearest historical earthquakes larger than the 17 May 2012 Timpson event are more than 400 km distant; e.g., in Oklahoma earthquakes with magnitudes of 5.5, 5.7, and 5.6 occurred in 1882, 1952, and 2011.

The magnitudes of both the 17 May 2012 earthquake and 10 May foreshock were adjusted upward several days after they occurred. That is, the 17 May magnitude was initially reported as m_{bGS}4.3 from short-period body waves, and the 10 May foreshock magnitude as m_{bGS}3.7. Then, following analysis of broadband regional signals to determine the scalar moments and focal mechanisms for both events, the magnitudes were upgraded to $M_{W\text{-RMT}}$4.8 and $M_{W\text{-RMT}}$3.9. This suggests that the body-wave amplitudes at frequencies of ~1 s used to determine m_{bGS} give magnitude values somewhat smaller than predicted by the *Atkinson and Boore* [2006; 2011] Central U.S. strong motion model. It also suggests that the magnitudes cataloged for some historical earthquakes in East Texas and along the Gulf Coastal Plain—determined from body waves—might be smaller than moment magnitudes that might have been determined using modern methods had broadband observations been available.

References

Aki, K. (1965), Maximum likelihood estimate of b in the formula log N = A–bM and its confidence limits, *Bull. Res. Inst. Tokyo Univ.*, *43*, 237–239.

Aki, K., and P. G. Richards (1980), *Quantitative Seismology*, Freeman and Co., San Francisco, Calif.

Atkinson, G. M., and D. M. Boore (2006), Earthquake ground-motion prediction equations for eastern North America, *Bull. Seismol. Soc. Am.*, *96*, 2181–2205.

Atkinson, G. M., and D. M. Boore (2011), Modifications to existing ground-motion prediction equations in light of new data, *Bull. Seismol. Soc. Am.*, *101*, 1121–1135.

Atkinson, G. M., and D. J. Wald (2007), "Did you feel it"? intensity data: A surprisingly good measure of earthquake ground motion, *Seismol. Res. Lett.*, *78*, 362–368, doi:10.1785/gssrl.78.3.362.

Davis, S. D., P. Nyffenegger, and C. Frohlich (1995), The 9 April 1993 earthquake in south-central Texas: Was it induced by fluid withdrawal?, *Bull. Seismol. Soc. Am.*, *85*, 1888–1895.

Ekström, G., M. Nettles, and A. M. Dziewonski (2012), The global CMT project 2004–2010: Centroid-moment tensors for 13,017 earthquakes, *Phys. Earth Planet. Inter.*, *200–201*, 1–9, doi:10.1016/j.pepi.2012.04.002.

Ellsworth, W. L. (2013), Injection-induced earthquakes, *Science*, *341*, 1225924, doi:10.1126/science.1225942.

Ewing, T. (1990), *Tectonic Map of Texas*, Univ. Texas Bureau of Economic Geology, Austin, Tex.

Frohlich, C. (2012), Two-year survey comparing earthquake activity and injection-well locations in the Barnett Shale, Texas, *Proc. Natl. Acad. Sci. U.S.A.*, *109*, 13,934–13,938, doi:10.1073/pnas.1207728109.

Frohlich, C., and M. Brunt (2013), Two-year survey of earthquakes and injection/production wells in the Eagle Ford Shale, Texas, prior to the M_W4.8 20 October 2011 earthquake, *Earth Planet. Sci. Lett.*, *379*, 53–63, doi:10.1016/j.epsl.2013.07.02.

Frohlich, C., and S. D. Davis (2002), *Texas Earthquakes*, pp. 275, Univ. Texas Press, Austin, Tex.

Frohlich, C., C. Hayward, B. Stump, and E. Potter (2011), The Dallas-Fort Worth earthquake sequence: October 2008 through May 2009, *Bull. Seismol. Soc. Am.*, *101*, 327–340, doi:10.1785/0120100131.

Galloway, W. E., T. E. Ewing, C. M. Garrett, N. Tyler, and D. G. Bebout (1983), *Atlas of Major Texas Oil Reservoirs*, pp. 139, Univ. Texas Bureau Economic Geol, Austin, Tex.

Geomap Company (2012), Executive reference map 302: East Texas, scale 1:386,000, Dallas, Tex.

Hammes, U., H. S. Hamlin, and T. E. Ewing (2011), Geologic analysis of Upper Jurrasic Haynesville shale in East Texas and west Louisiana, *AAPG Bull.*, *95*, 1643–1666, doi:10.1306/02141110128.

Healy, J. H., W. W. Rubey, D. T. Griggs, and C. B. Raleigh (1968), The Denver earthquakes, *Science*, *161*, 1301–1310.

Herrmann, R. B., and S.-K. Park (1981), The Denver earthquakes of 1967–1968, *Bull. Seismol. Soc. Am.*, *71*, 731–745.

Herrmann, R. B., H. Benz, and C. J. Ammon (2011), Monitoring the earthquake source process in North America, *Bull. Seismol. Soc. Am.*, *101*, 2609–2625, doi:10.1785/0120110095.

Horton, S. (2012), Disposal of hydrofracking waste fluid by injection into subsurface aquifers triggers earthquake swarm in central Arkansas with potential for damaging earthquake, *Seismol. Res. Lett.*, *83*, 250–260, doi:10.1785/gssrl.83.2.250.

Jackson, M. P. A. (1982), *Fault Tectonics of the East Texas Basin*, Geol. Circular, vol. 82–4, p. 31, Univ. Texas Bureau Economic Geol., Austin, Tex.

Justinic, A. H., B. Stump, C. Hayward, and C. Frohlich (2013), Analysis of the Cleburne, Texas, earthquake sequence from June 2009 to June 2010, *Bull. Seismol. Soc. Am.*, *103*, 3083–3093, doi:10.1785/0120120336.

Keranen, K. M., H. M. Savage, G. A. Abers, and E. S. Cochran (2013), Potentially induced earthquakes in Oklahoma, USA: Links between wastewater injection and the M_W 5.7 earthquake sequence, *Geology*, *41*, 609–702, doi:10.1130/G34045.1.

Kim, W.-Y. (2013), Induced seismicity associated with fluid injection into a deep well in Youngstown, Ohio, *J. Geophys. Res. Solid Earth*, 3506–3518, doi:10.1002/jgrb.50247.

Kissling, E., W. L. Ellsworth, D. Eberhart-Phillips, and U. Kradolfer (1994), Initial reference models in local earthquake tomography, *J. Geophys. Res.*, *99*, 19,635–19,646.

Kosters, E. C., D. G. Bebout, S. J. Seni, C. M. Garrett, L. F. Brown, H. S. Hamlin, S. P. Dutton, S. C. Ruppel, R. J. Finley, and N. Tyler (1989), *Atlas of Major Texas Gas Reservoirs*, p. 161, Univ. Texas Bur. Econ. Geol, Austin, Tex.

Lutter, W. J., and R. L. Novack (1990), Inversion for crustal structure using reflections from the PASSCAL Ouachita experiment, *J. Geophys. Res.*, *95*, 4633–4646.

Pennington, W. D., and S. M. Carlson (1984), *Observations From the East Texas Seismic Network (June 1981–August 1982)*, vol. 84–3, p. 48, Univ. Texas, Bureau Economic Geol. Circ. 84-3, Austin, Tex.

Acknowledgments

We are indebted to the property owners who graciously allowed us to install and operate seismographs on private property. We thank David Wald and Vince Quitoriano, who provided did-you-feel-it (DYFI) information for constraining the MMI III and MMI IV intensity areas, allowing us to focus our field studies in the higher-intensity areas. We thank Julia Gale and Martin Jackson for providing valuable information about regional geology and Wayne Pennington, Art McGarr, Andrea Llenos, and an anonymous reviewer for helpful suggestions that improved the manuscript. This research was partially supported by the USGS, Department of the Interior, under USGS award G12AP20001 and G13AP00023; and by Research Partnership to Secure Energy for America (RPSEA) subcontract 11122-27 through the "Ultra-Deepwater and Unconventional Natural Gas and Other Petroleum Resources" program authorized by the U.S. Energy Policy Act of 2005. RPSEA (www.rpsea.org) is a nonprofit corporation whose mission is to provide a stewardship role in ensuring the focused research, development, and deployment of safe and environmentally responsible technology that can effectively deliver hydrocarbons from domestic resources to the citizens of the United States. RPSEA, operating as a consortium of premier U.S. energy research universities, industry, and independent research organizations, manages the program under a contract with the U.S. Department of Energy's National Energy Technology Laboratory. The views and conclusions contained in this document are those of the authors and should not be interpreted as representing the official policies, either expressed or implied, of the U.S. Government.

Pennington, W. D., S. D. Davis, S. M. Carlson, J. Dupree, and T. E. Ewing (1986), The evolution of seismic barriers and asperities caused by the depressuring of fault planes in oil and gas fields of south Texas, *Bull. Seismol. Soc. Am.*, *76*, 939–948.

Wald, D. J., V. Quitoriano, B. Worden, M. Hopper, and J. W. Dewey (2011), USGS "Did you feel it?" internet-based macroseismic intensity maps, *Ann. Geophys.*, *54*, 688–707, doi:10.4401/ag-5354.

Zhu, L., and L. A. Rivera (2002), A note on the dynamic and static displacements from a point source in multilayered media, *Geophys. J. Int.*, *148*, 619–627.